

## Roles of four feedback loops in mitochondrial permeability transition pore opening induced by $\text{Ca}^{2+}$ and reactive oxygen species

Hong Qi <sup>1,2,\*</sup> Guoping Xu,<sup>1,2</sup> Xiao-Long Peng <sup>1,2</sup> Xiang Li,<sup>3,4</sup> Jianwei Shuai,<sup>3,4,5</sup> and Rui Xu<sup>1,2,†</sup>

<sup>1</sup>Complex Systems Research Center, Shanxi University, Taiyuan 030006, China

<sup>2</sup>Shanxi Key Laboratory of Mathematical Techniques and Big Data Analysis on Disease Control and Prevention, Shanxi University, Taiyuan 030006, China

<sup>3</sup>Department of Physics, College of Physical Science and Technology, Xiamen University, Xiamen 361005, China

<sup>4</sup>State Key Laboratory of Cellular Stress Biology, Innovation Center for Cell Signaling Network, Xiamen University, Xiamen 361102, China

<sup>5</sup>National Institute for Data Science in Health and Medicine, Xiamen University, Xiamen 361102, China



(Received 2 June 2020; accepted 4 December 2020; published 23 December 2020)

Transient or sustained permeability transition pore (PTP) opening is important in normal physiology or cell death, respectively. These are closely linked to  $\text{Ca}^{2+}$  and reactive oxygen species (ROS). The entry of  $\text{Ca}^{2+}$  into mitochondria regulates ROS production, and both  $\text{Ca}^{2+}$  and ROS trigger PTP opening. In addition to this feedforward loop, there exist four feedback loops in the  $\text{Ca}^{2+}$ -ROS-PTP system. ROS promotes  $\text{Ca}^{2+}$  entering (F1) and induces further ROS generation (F2), forming two positive feedback loops. PTP opening results in the efflux of  $\text{Ca}^{2+}$  (F3) and ROS (F4) from the mitochondria, forming two negative feedback loops. Owing to these complexities, we construct a mathematical model to dissect the roles of these feedback loops in the dynamics of PTP opening. The qualitative agreement between simulation results and recent experimental observations supports our hypothesis that under physiological conditions the PTP opens in an oscillatory state, while under pathological conditions it opens in a high steady state. We clarify that the negative feedback loops are responsible for producing oscillations, wherein F3 plays a more prominent role than F4; whereas the positive feedback loops are beneficial for maintaining oscillation robustness, wherein F1 has a more dominant role than F2. Furthermore, we manifest that the proper increase in negative feedback strength or decrease in positive feedback strength not only facilitates the occurrence of oscillations and thus protects the system against a high steady state, but also assists in lowering the oscillation peak. This study may provide potential therapeutic strategies in treating neurodegenerative diseases due to PTP dysfunction.

DOI: [10.1103/PhysRevE.102.062422](https://doi.org/10.1103/PhysRevE.102.062422)

### I. INTRODUCTION

In addition to the well-known role of mitochondria in energy metabolism, regulation of cell death has now emerged as a second important function of these organelles [1]. These are intimately linked to calcium ions ( $\text{Ca}^{2+}$ ) and reactive oxygen species (ROS). Under physiological conditions, entry of an appropriate amount of  $\text{Ca}^{2+}$  into the mitochondria activates key enzymes involved in tricarboxylic acid cycle to produce adenosine triphosphate (ATP) by oxidative phosphorylation, which is necessary for cell survival [2,3]. While under pathological conditions, exaggerated  $\text{Ca}^{2+}$  influx into the mitochondria induces the production of a large amount of ROS, and together cause the sustained opening of permeability transition pore (PTP), thereby leading to cell death [4,5]. The opening of PTP has been linked to the pathology of neurodegenerative diseases, where the sustained PTP opening induces excessive cell death and brain tissue damage [6–9].

However, there is an emerging theme that PTP opening does not always lead to cell death and, instead, has im-

portant physiological functions in  $\text{Ca}^{2+}$  homeostasis, ROS signaling, cell development, and cellular metabolism [10–12]. Actually, the PTP can operate under two distinct modes: low-conductance state associated with transient opening and high-conductance state associated with persistent opening [13–16]. The transient opening of PTP is typically a reversible and repetitive event [14,17,18] with frequency of 1 ~ 11 times per minute [19], which plays a physiological role in many cellular processes [20]. In contrast, the persistent opening of PTP is irreversible [15], which results in increased mitochondrial permeability to ions and solutes, followed by organelle swelling and disruption of the mitochondrial membrane, and cell death [21]. According to these experimental observations, the PTP can impact the cell fate decisions in a dichotomous manner, dependent upon the mode of PTP opening. From a dynamical point of view, these results allow us to put forward a hypothesis that, under physiological conditions the PTP opens in a transient mode and this mode corresponds to an oscillatory state; whereas under pathological conditions the PTP opens in a persistent mode and this mode corresponds to a high steady state [Fig. 1(a)].

Thus, the dynamics of PTP opening is deserved to be studied in view of its significance in physiological and pathological conditions. It is generally recognized that  $\text{Ca}^{2+}$ , ROS, and PTP form a coherent feedforward loop with an AND input

\*Corresponding author: hongqi@sxu.edu.cn

†Corresponding author: xurui@sxu.edu.cn

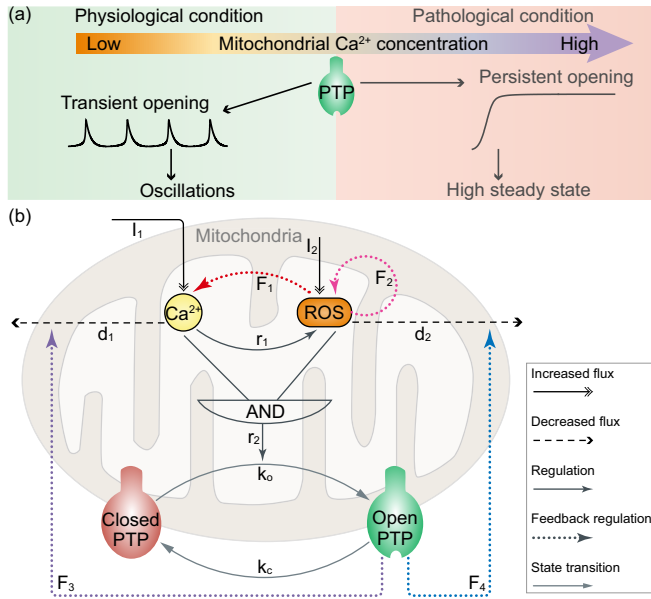


FIG. 1. Working hypothesis and schematic diagram. (a) Under physiological condition, a small amount of Ca<sup>2+</sup> facilitates transient opening of PTP; while under pathological condition, large amount of Ca<sup>2+</sup> promotes persistent opening of PTP. The transient opening mode and persistent opening mode correspond to the oscillatory state and high steady state, respectively. (b) The double-headed arrow for Ca<sup>2+</sup> indicates the influx of Ca<sup>2+</sup> into the mitochondria, for ROS indicates the basal synthesis of ROS. The dashed-line arrow for Ca<sup>2+</sup> represents the efflux of Ca<sup>2+</sup> from the mitochondria, for ROS represents the degradation of ROS. The regulatory effect of Ca<sup>2+</sup> on ROS as well as the combined regulatory effect of Ca<sup>2+</sup> and ROS on PTP are represented by the swallowtail arrow. Besides the regulatory effect, PTP opening occurs with a basal rate. PTP can switch between open state and closed state. The dotted-line arrows denote the four feedback loops. F<sub>1</sub> and F<sub>2</sub> are positive feedback loops, while F<sub>3</sub> and F<sub>4</sub> are negative feedback loops.

function [6], that is, Ca<sup>2+</sup> accumulation within mitochondria can enhance the generation of ROS [22], jointly triggering PTP opening [5,23]. However, feedback loops are pervasive in biological signaling system, and are instrumental in shaping the overall dynamic behavior of the system [24]. Indeed, accumulating evidence suggests that there exist four feedback loops in the Ca<sup>2+</sup>-ROS-PTP system [Fig. 1(b)]. During the ATP production, ROS are generated as a consequence of Ca<sup>2+</sup>-dependent oxidative phosphorylation [25,26], which in turn exert a positive feedback on Ca<sup>2+</sup> influx to the mitochondria (abbreviated as F<sub>1</sub>, see Supplemental Material for details [27]) [28,29]. ROS can induce further ROS generation, a process termed ROS-induced ROS generation [30,31], constituting a second positive feedback loop (abbreviated as F<sub>2</sub>). Although Ca<sup>2+</sup> and ROS cooperate to promote the opening of PTP [32], which allows free passage of molecules up to 1.5 kDa in size, PTP opening results in the efflux of Ca<sup>2+</sup> and ROS from the mitochondria [14,33], thus forming two negative feedback loops, abbreviated as F<sub>3</sub> and F<sub>4</sub>, respectively.

The presence of multiple feedback loops in the Ca<sup>2+</sup>-ROS-PTP system poses a challenge to quantitatively disentangle the relative contributions of each feedback loop to the oscillatory

behavior of the PTP, and to explore how to prevent the PTP from an oscillatory state into a high steady state. We examine the mechanisms underlying the dynamics of PTP opening using robustness analysis and bifurcation analysis. We clarify that while the negative feedback loops are fundamental in generating oscillations, the positive feedback loops are critical for maintaining robustness of the oscillations. Furthermore, we demonstrate that F<sub>3</sub> (or F<sub>1</sub>) plays a more important role than F<sub>4</sub> (or F<sub>2</sub>) in generating oscillations. In addition, we manifest that the appropriate increase in negative feedback strength or decrease in positive feedback strength not only facilitates the occurrence of oscillations and thus prevents the system from keeping in a high steady state, but also contributes to reducing the peak values of the oscillations. This study reveals the roles of the four feedback loops in the Ca<sup>2+</sup>-ROS-PTP system and may provide therapeutic strategies for prevention or treatment of neurodegenerative diseases such as Alzheimer's and Parkinson's diseases.

## II. MODEL

To investigate qualitatively the dynamics of PTP opening, we develop a coarse-grained phenomenological model based on the following two considerations. On one hand, the generation of ROS involves multiple steps and thus needs dozens of ordinary differential equations (ODEs) to describe these steps, which will make the situation very complex. On the other hand, the underlying mechanisms causing the opening of PTP by Ca<sup>2+</sup> and ROS are not fully understood. The detailed biological background of the mathematical model can be found in Supplemental Material [27]. The simplified system comprises three constituents: Ca<sup>2+</sup>, ROS, and PTP [Fig. 1(b)]. The dynamics of the system is determined by three coupled ODEs

$$\frac{dC}{dt} = I_1 - d_1C + F_1 \frac{R^4}{k_{RC}^4 + R^4} - F_3 \frac{P^4}{k_{PC}^4 + P^4} C, \quad (1a)$$

$$\begin{aligned} \frac{dR}{dt} = & I_2 - d_2R + r_1 \frac{C^4}{k_{CR}^4 + C^4} + F_2 \frac{R^4}{k_{RR}^4 + R^4} \\ & - F_4 \frac{P^4}{k_{PR}^4 + P^4} R, \end{aligned} \quad (1b)$$

$$\frac{dP}{dt} = \left( k_o + r_2 \frac{C^4}{k_{CP}^4 + C^4} \frac{R^4}{k_{RP}^4 + R^4} \right) (1 - P) - k_c P, \quad (1c)$$

where  $C$  and  $R$  are the amount of Ca<sup>2+</sup> and ROS, respectively;  $P$  is the fraction of open PTP.

Mitochondrial Ca<sup>2+</sup> uptake is controlled by mitochondrial calcium uniporter (MCU), while extrusion is mainly mediated by Na<sup>+</sup>-Ca<sup>2+</sup> exchanger [34]. The first term in Eq. (1a) corresponds to an average influx rate during the opening of MCU. The second term in Eq. (1a) corresponds to the rate of Ca<sup>2+</sup> extrusion, which is described by a linear function.

The basal synthesis rate of ROS can be expressed as a constant and the degradation rate is proportional to its amount. The positive effect of Ca<sup>2+</sup> on ROS synthesis is modeled using Hill-type kinetics, which is due to the multistep processing of ROS production and strong cooperativity in this process [22]. These are described by the first three terms of Eq. (1b).

The last two terms of Eqs. (1a) and (1b) represent the four feedback loops. We assume that the two positive feedback loops are represented by Hill function, and the two negative feedback loops are represented by the product of a Hill function and the amount of  $\text{Ca}^{2+}$  or ROS available to be released.

Equation (1c) has one term for PTP opening and a second for its closure. The rate of PTP closure is proportional to the fraction of open PTP,  $P$ . Conversely, the rate of PTP opening is proportional to the fraction of closed PTP ( $1 - P$ ). The constitutive opening of PTP in the absence of stimulation is in line with its involvement in mediating important physiologic functions [10,14]. In addition, mitochondrial  $\text{Ca}^{2+}$  overload and excessive ROS are the key triggers for PTP opening [35], so the joint activating effect of  $\text{Ca}^{2+}$  and ROS on closed PTP is expressed as the product of two Hill-type functions.

It should be pointed out that the reasons why we employ seven Hill functions can be summarized into two categories. First, an ultrasensitive response, which increases multiplicatively with the number of reaction steps, is often empirically approximated by the Hill function [36,37]. Second, the unknown biological process is generally approximated by the Hill function, because the Hill equation is very powerful in its ability to fit the input-output patterns of diverse biological processes [38]. The detailed aspects of the biological reactions covered in the current model are provided in the biological background section of Supplemental Material [27]. For simplicity, all Hill coefficients are assumed to be identically equal to 4. However, we also validate our conclusion under different Hill coefficients [Figs. S2(a) and S2(b)]. In addition, to verify that the choice of specific function does not affect the conclusion, we also use bilinear kinetics to model the efflux mechanism of  $\text{Ca}^{2+}$  and ROS from the PTP [Fig. S2(c)].

The meaning of each parameter and its corresponding standard value are listed in Table S1. As a fact, most of the reaction progresses in the model represent the interactive relationships, which are the combinations of several chemical reactions, so most of the parameters are lumped parameters which do not have physiologically realistic values. It should be noted that although the concentration of  $\text{Ca}^{2+}$  in the mitochondria has been determined experimentally, the precise concentration of ROS remains unresolved because of its high reactivity and short half-life [39,40]. For convenience, we choose the values

of parameters so that the amount of  $\text{Ca}^{2+}$  and ROS can largely be restricted between 0 and 1.  $P$ , the fraction of open PTP, is regarded as the output of the system.

### III. RESULTS

#### A. Eleven out of twelve modes can exhibit oscillatory behavior

Every feedback loop may be present or absent, resulting in  $2^4 = 16$  kinds of topologies. Since the PTP should be in an oscillatory state under physiological conditions, we first seek to determine the roles of each feedback loop in the oscillatory behavior of PTP. Many studies have demonstrated that the existence of at least one negative feedback loop is a necessary condition for producing sustained oscillations [41–44]. In this scenario, there are 12 theoretically possible oscillatory topologies [termed mode FX, see Fig. 2], except for four modes without any negative feedback loop.

The dynamical behavior of each mode is determined by its corresponding ODEs, which can be obtained by setting certain  $F_X$  ( $X = 1, 2, 3, 4$ ) to zero in the overall system. So the number of parameters of different mode is between 12 and 19, depending on the mode topology. We properly select a particular set of kinetic parameters for each mode (Tables S1 and S2) to identify the modes that could result in PTP oscillations. From the time series of  $P$  in Fig. 2, one can see that except mode F4, all the other 11 modes can really generate oscillations.

For mode F4, when the Hill coefficients are chosen as any positive integer, system (1a)–(1c) reduces to the following ODEs:

$$\frac{dC}{dt} = I_1 - d_1 C, \quad (2a)$$

$$\frac{dR}{dt} = I_2 - d_2 R + r_1 \frac{C^n}{k_{CR}^n + C^n} - F_4 \frac{P^n}{k_{PR}^n + P^n} R, \quad (2b)$$

$$\frac{dP}{dt} = \left( k_o + r_2 \frac{C^n}{k_{CP}^n + C^n} \frac{R^n}{k_{RP}^n + R^n} \right) (1 - P) - k_c P. \quad (2c)$$

Since we focus on the steady-state behavior of the system, we can obtain from Eq. (2a) that  $C = I_1/d_1$ . On substituting it into Eqs. (2b) and (2c), the system reduces to

$$\begin{aligned} \frac{dR}{dt} &= I_2 - d_2 R + r_1 \frac{(I_1/d_1)^n}{k_{CR}^n + (I_1/d_1)^n} - F_4 \frac{P^n}{k_{PR}^n + P^n} R \\ &\triangleq X(R, P), \\ \frac{dP}{dt} &= \left( k_o + r_2 \frac{(I_1/d_1)^n}{k_{CP}^n + (I_1/d_1)^n} \frac{R^n}{k_{RP}^n + R^n} \right) (1 - P) - k_c P \\ &\triangleq Y(R, P). \end{aligned}$$

Choosing a Dulac function  $B(R, P) = 1$ , we have

$$\frac{\partial(BX)}{\partial R} + \frac{\partial(BY)}{\partial P} = -d_2 - F_4 \frac{P^n}{k_{PR}^n + P^n} - \left( k_o + r_2 \frac{(I_1/d_1)^n}{k_{CP}^n + (I_1/d_1)^n} \frac{R^n}{k_{RP}^n + R^n} \right) - k_c < 0.$$

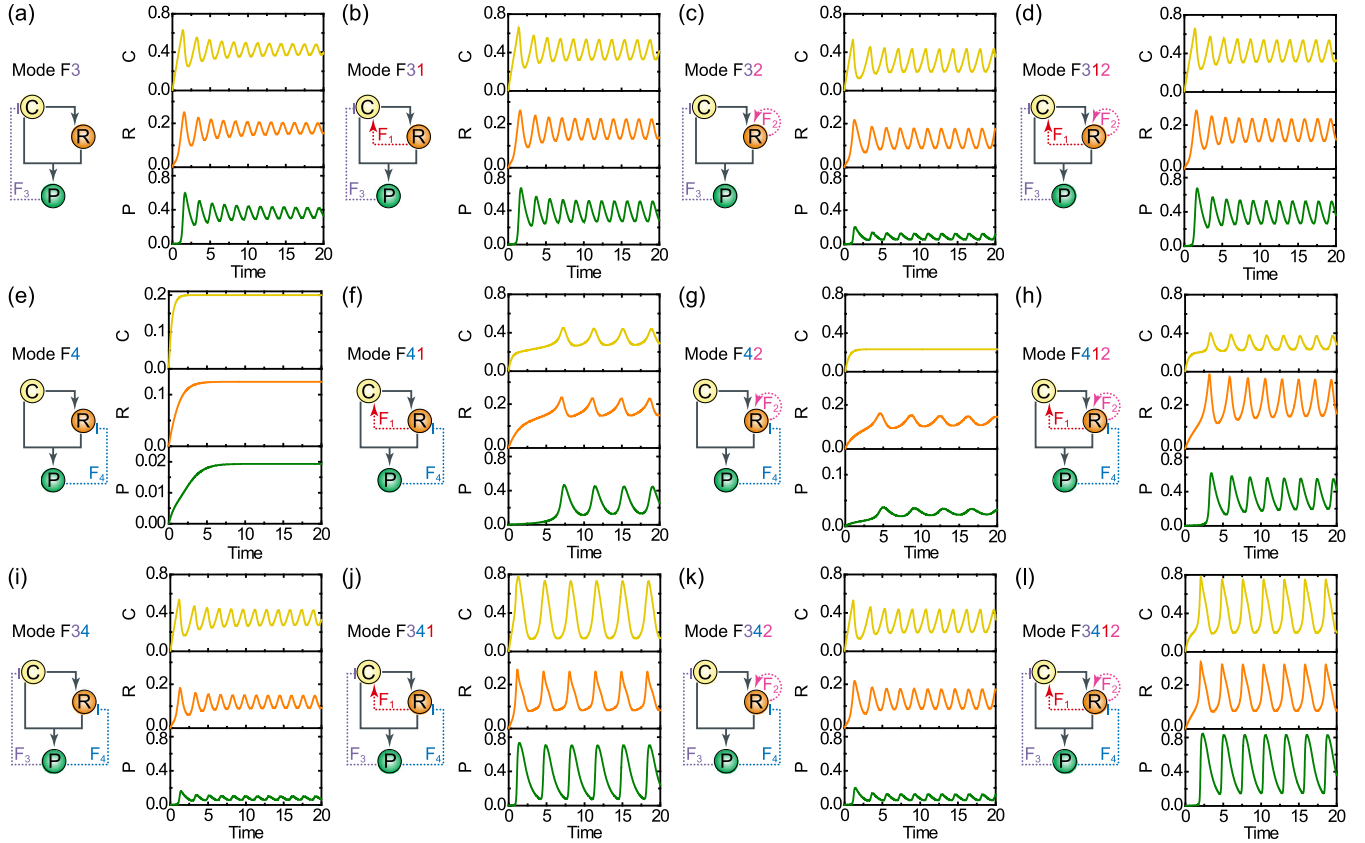


FIG. 2. (a)–(l) Time course of 12 modes. For the schematic diagrams (left), solid lines indicate regulatory interactions that are present in all of the topologies, while dashed lines indicate the ones that maybe present or absent, depending on topology. Representative examples of time course of three variables (right). C,  $\text{Ca}^{2+}$ ; R, ROS; P, the fraction of open PTP. The unit is arbitrary.

According to the Bendixson-Dulac criterion [45], this system has no periodic solutions and therefore mode F4 will not give rise to oscillations.

### B. Effects of feedback loops in oscillatory behavior—From a robustness view point

To discern the relative contribution of each feedback loop in the oscillatory behavior of PTP, we estimate the functional robustness [46,47] of the 12 modes. The functional robustness is measured by the percentage  $p = m/n$ , where  $n$ , being equal to  $10^6$ , is the number of random parameter sets used in the sampling and  $m$  is the number of those that can produce sustained oscillations. For reducing the computational cost and time, two decreased rates ( $d_1$  and  $d_2$ ) and four half-saturation constants related to feedback loops ( $K_{RC}$ ,  $K_{PC}$ ,  $K_{RR}$ , and  $K_{PR}$ ) are assumed to vary while the other parameters are fixed. The ranges of the six parameters used in the sampling are listed in Table S1. We use linear sampling in the study, and for each sampling, the six parameters are selected independently. During a long-time simulation, if sustained oscillations are detected, this randomly chosen parameter set will be recognized as a parameter set that yielded sustained oscillations.

Figure 3(a) shows the percentage of randomly chosen parameter sets that yielded sustained oscillations for the 12 modes. At least three features are worth pointing out. First, the percentage  $p_{\text{Mode}}$  varies dramatically among different modes,

e.g.,  $p_{F4} = 0\%$ ,  $p_{F42} = 0.0004\%$ , and  $p_{F3412} = 28.7\%$ . Second, the modes with the two largest percentages are mode F341 and F3412, which consist of two negative feedback loops, i.e., F3 and F4 and one positive feedback loop, i.e., F1. Third,  $p_{\text{Mode}}$  is larger for the modes containing F3 than the modes containing F4, and  $p_{\text{Mode}}$  is larger for the modes containing F1 than those containing F2.

There are four modes including two negative feedback loops (F34, F341, F342,e and F3412) and three modes including two positive feedback loops (F312, F412, and F3412). To dissect the relative contribution of individual feedback loops within a certain feedback type to oscillatory behavior of PTP, we compare the probability due to the presence of this feedback loop in these hybrid modes. For the mode F341,  $p_{F341} = 25\%$  yields oscillations. If we block F4 in this mode,  $20\% p_{F341}$  parameter sets yields oscillations, while if we block F3, only about  $4\% p_{F341}$  parameter sets yields oscillations; the remaining  $76\% p_{F341}$  parameter sets yielded oscillations are owing to the presence of both F3 and F4. As shown in Fig. 3(b), most of the parameter combinations yielded oscillations are as a result of the existence of F3. Thus, compared to F4, F3 is the dominant mechanism for producing oscillations. Similarly, compared to F2, F1 is the dominant mechanism for producing oscillations [Fig. 3(c)].

Having assessed the influence of feedback loops on the robustness of the oscillatory behavior of PTP, we then focus on their impact on peak value, which is an important feature

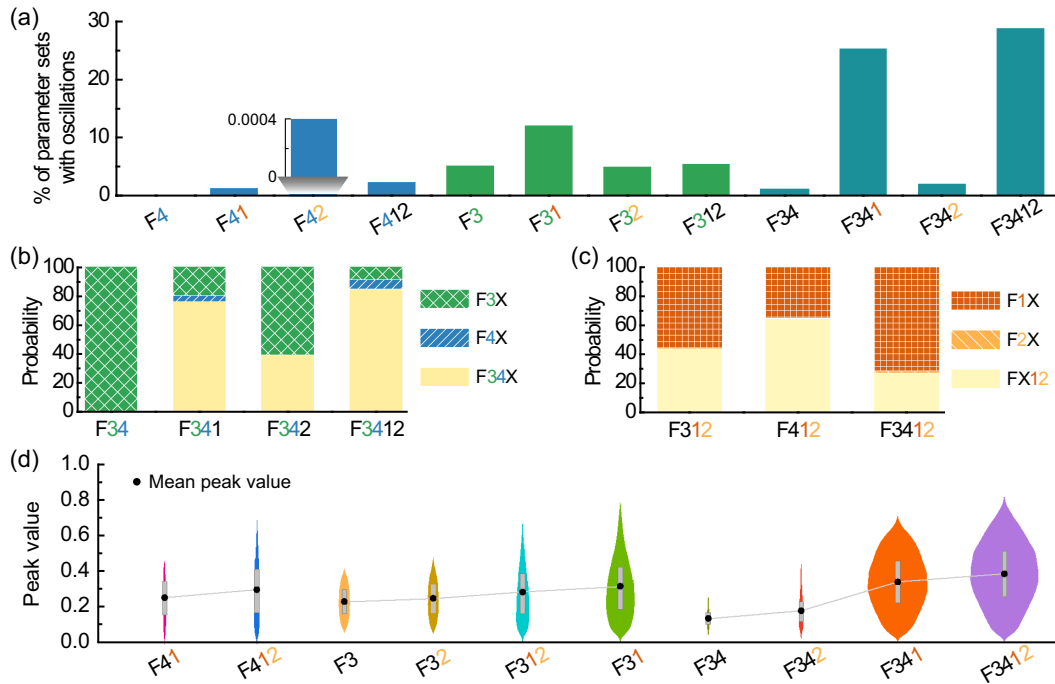


FIG. 3. Robustness properties of 12 modes. (a) Percentage of parameter sets that yielded sustained oscillations. (b) and (c) Probability of parameter sets that yielded sustained oscillations thanks to the presence of specified feedback loop(s). (d) The distribution of peak values of ten modes. Violin plots show mean, 25th and 75th percentiles; sample sizes are represented by the widths.

of oscillation. The violin plots shown in Fig. 3(d) display the distribution of the peak value for ten modes where at least 7868 (the number of mode F<sub>34</sub>) parameter combinations yield sustained oscillations. The comparison indicates that, except modes F<sub>4</sub><sup>1</sup> and F<sub>4</sub><sup>12</sup>, the range of the peak value is largely proportional to their own  $p_{\text{Mode}}$ . Figure 3(d) reveals that the peak value is significantly high when the mode includes a positive feedback loop, and that the peak value is significantly higher in modes with F<sub>1</sub> relative to modes with F<sub>2</sub>. Therefore, the two positive feedback loops result in the increase of the peak value of the oscillatory system. Notably, F<sub>1</sub> has an outsized influence on producing oscillations with large peak value.

From Figs. 3(a) and 3(d) we can see that mode F<sub>34</sub><sup>12</sup>, consisting of two positive feedback loops and two negative feedback loops, not only owns the highest percentage in producing oscillations, but also permits these oscillations over a wide range of amplitude. Thus mode F<sub>34</sub><sup>12</sup> displays greater robustness than the other 11 modes. This suggests that mode F<sub>34</sub><sup>12</sup> is a most favorable circuit used in biological systems because robustness is believed to be an essential property of biological systems [48]. A robust mode must own different amplitude sensitivities and thus satisfy cell-, tissue- or organism-specific demands by only adapting reaction velocities while keeping the circuit structure unchanged [49].

### C. Effects of feedback loops in dynamical behavior—From a bifurcation view point

To test our hypothesis that PTP opens in an oscillatory state under physiological conditions while it opens in a high steady state under pathological conditions, and further investigate

the influence of the feedback loops on this transition, the methods of bifurcation analysis were employed. The mode F<sub>34</sub><sup>12</sup>, which is suggested as the most suitable circuit used in biological systems, is selected as an illustrative example to demonstrate the results.

Starting with the bifurcation diagram of  $P$  with  $I_1$ , the basal rate of  $\text{Ca}^{2+}$  uptake into the mitochondria, as the control parameter, we investigate the influence of the influx of  $\text{Ca}^{2+}$  into the mitochondria on PTP opening. Figure 4 shows that when  $I_1$  is small, PTP opens in an oscillatory manner with low mean value, but when  $I_1$  is beyond a critical level about 0.6 (which is called a bifurcation point), PTP opens in a permanent manner with high value. As a result, the increased influx of  $\text{Ca}^{2+}$  into the mitochondria can change the PTP opening mode from an oscillatory state to a high steady state. The simulation result is qualitatively consistent with the experimental observations [14,16,17], which show that under physiological conditions, a small amount of  $\text{Ca}^{2+}$  enters into the mitochondria and PTP operates in a transient and low-conductance mode; while under pathological conditions, a substantial amount of  $\text{Ca}^{2+}$  influxes into the mitochondria and then causes PTP opening in a persistent and high-conductance mode. Accordingly, the oscillation and high steady-state regions are corresponding to the physiological and pathological conditions, respectively.

The bifurcation point in Fig. 4 indicates the transition from an oscillatory state to a high stable steady state, which represents the point of no return in cell commitment to death [50]. The shift of the bifurcation point is a good measure for describing cell fate conversion compared with the original condition. In detail, if this point moves towards a lower value of the control parameter, the oscillatory domain is shrunk and

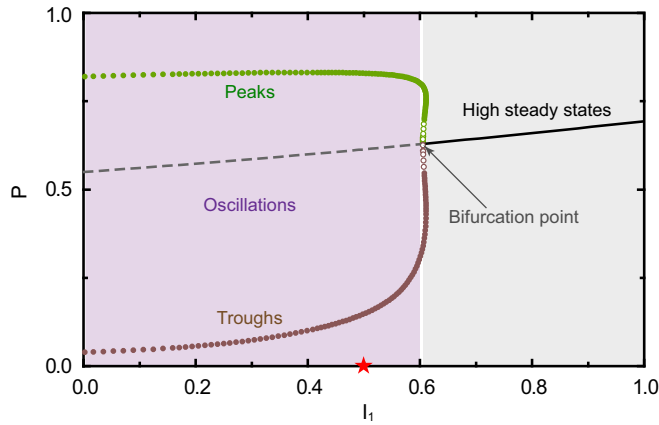


FIG. 4. Bifurcation diagram of  $P$  as a function of  $I_1$ . The intersection of solid and dashed lines is a bifurcation point. The solid and dashed line indicate, respectively, stable and unstable solutions of the ordinary differential equations corresponding to mode F3412. Each unstable solution is surrounded by a stable oscillation, the peak and trough of which are indicated by a green and brown filled circle, respectively. The unstable oscillations are represented by empty circles. The standard value of  $I_1$  is marked by an asterisk.  $I_1$ , basal rate of  $Ca^{2+}$  uptake into mitochondria.

the cell will survive in a narrower range of conditions; if it moves towards a higher value of the control parameter, the oscillatory domain is enlarged and the cell will survive in a wider range of conditions.

Next, we explore the effects of the four feedback loops on the shift of the bifurcation point. The feedback strength of the individual loops can be adjusted by varying the maximal

rate of the corresponding Hill function, i.e.,  $F_X$  ( $X = 1, 2, 3, 4$ ) listed in Table S1. Each subfigure in Fig. 5 shows the bifurcation diagrams of  $P$  with respect to  $I_1$  when the feedback strength  $F_X$  is increased or decreased by 10%. As shown in Fig. 5(a), one can see that compared with the bifurcation point obtained by the standard parameter  $F_1$ , the increased  $F_1$  results in a leftward shift of bifurcation point, while the decreased  $F_1$  results in a rightward shift. The leftward shift of the bifurcation point means that the death threshold becomes lower and cells are more prone to die. Conversely, the rightward shift of the bifurcation point means that the death threshold becomes higher and cells are more prone to survive. Figure 5(b) shows that  $F_2$  has a similar effect on the shift of the bifurcation point as  $F_1$ .  $F_3$  and  $F_4$  bring about the opposite effect in this regard [Figs. 5(c) and 5(d)].

As the oscillatory PTP opening is often associated with physiological conditions, while persistent PTP opening is often associated with pathological conditions, we then analyze how the four feedback loops affect the dynamical behavior of the system. Figure 6 presents the bifurcation diagrams of  $P$  with  $F_X$  ( $X = 1, 2, 3, 4$ ) as the bifurcation parameter, showing that these feedback loops affect the dynamics differently. A higher strength of the positive feedback loops,  $F_1$  and  $F_2$ , tends to move the system out of the oscillatory domain [Figs. 6(a) and 6(b)], thereby promoting cell death, while a higher strength of the negative feedback loops,  $F_3$  and  $F_4$ , tends to drive the system into the oscillatory domain [Figs. 6(c) and 6(d)], thereby facilitating cell survival. The bifurcation diagrams of the other 10 modes (not shown) also demonstrate that they can generate similar dynamics behavior as obtained in the F3412 mode.

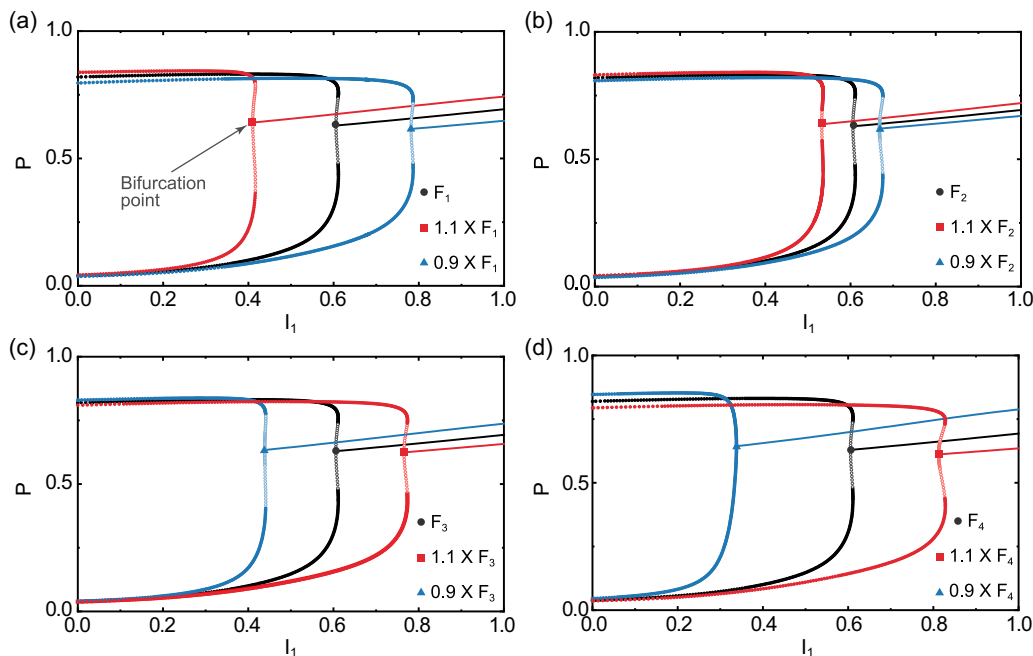


FIG. 5. Bifurcation diagrams of  $P$  as a function of  $I_1$  under different value of  $F_X$ .  $F_X$  ( $X = 1, 2, 3, 4$ ), maximal value of the corresponding feedback term, can represent the strength of feedback loop of mode F3412. In each subfigure, the black bifurcation diagram is the same as in Fig. 4 and is shown for facilitating comparison; the red or blue bifurcation diagram, respectively, corresponds to the situation when  $F_X$  is increased or decreased by 10%. The graphical notations are similar as in Fig. 4.  $I_1$ , basal rate of  $Ca^{2+}$  uptake into mitochondria.

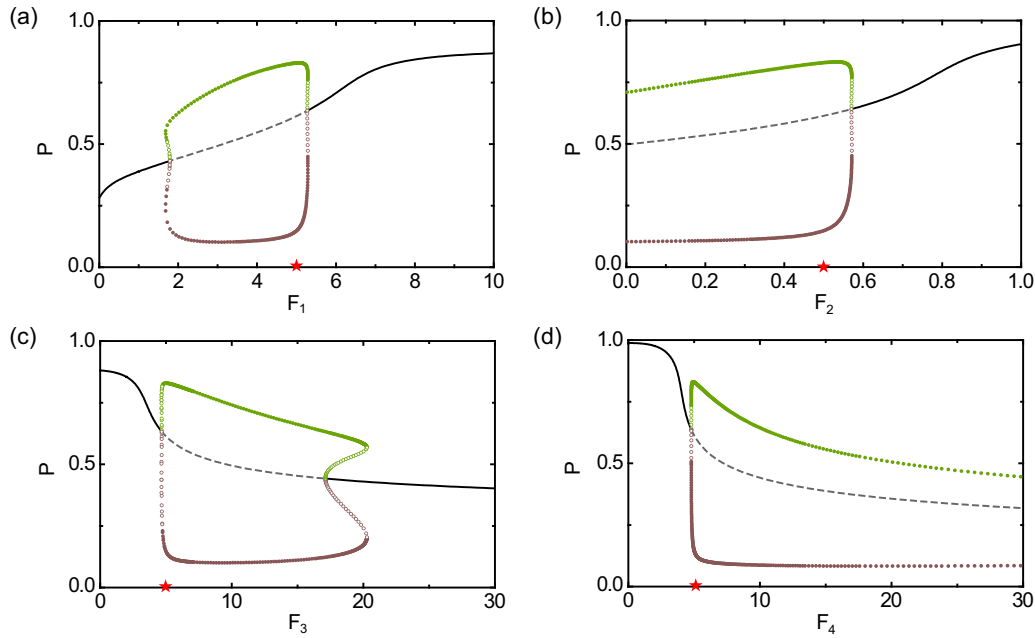


FIG. 6. Bifurcation diagrams of  $P$  as a function of  $F_X$ . The graphical notations are the same as in Fig. 4.  $F_X$  ( $X = 1, 2, 3, 4$ ), maximal value of the corresponding feedback term, can represent the strength of feedback loop of mode F3412. The detailed meaning and standard value (marked by an asterisk) of  $F_X$  are listed in Table S1.

More holistic view on the dynamic behavior of the system with respect to the feedback loops can be characterized by the bifurcation diagram when two feedback strengths are varied simultaneously. The two-parameter bifurcation diagram based on  $F_1$  and  $F_2$  suggests that an oscillatory region can be obtained for intermediate  $F_1$  and small  $F_2$ , and that the peak value increases with stronger feedback strength of  $F_1$  and  $F_2$ , of which  $F_1$  seems to play a more significant role [Fig. 7(a)]. The two-parameter bifurcation diagram based on  $F_3$  and  $F_4$  suggests that the oscillatory behavior arise if they exceed a certain value, and that the peak value increases with weaker feedback strength of  $F_3$  and  $F_4$  [Fig. 7(b)]. For modes F312 and F412 as well as modes F34, F341, and F342 (not shown), we have the same conclusions.

Since the choice of the parameter values in our model is to some extent arbitrary, we finally perform the parameter sensitivity analysis to evaluate the robustness of parameter-dependent mode F3412. Because we focus on the oscillatory behavior, which is corresponding to physiologically relevant states, we vary each parameter individually in a range from 0.1-fold to twofold of its standard value to inquire whether the applied perturbation still maintains the oscillations. As indicated in Fig. 8, the presence or absence of a circle represents, respectively, that the oscillations can be guaranteed or not guaranteed, so the number of the circles captures the role of each parameter in preserving the oscillatory nature of PTP opening. For instance, the standard value of  $I_1$  is 0.5 (Table S1); oscillations still occur if it is reduced to 0.05 or

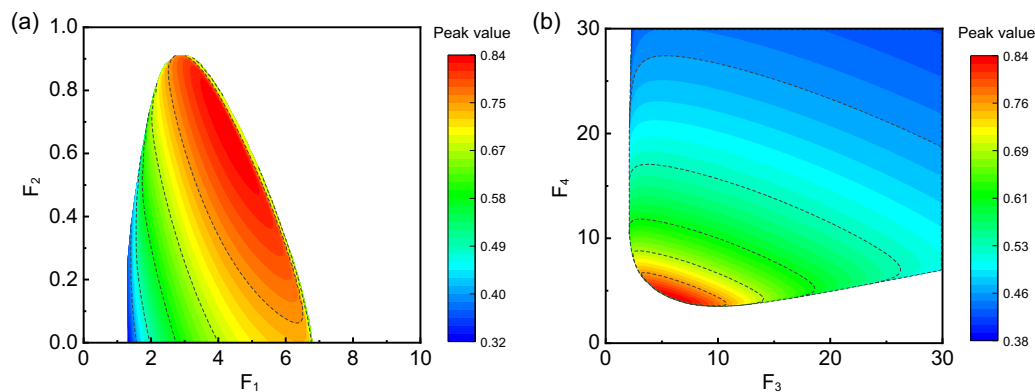


FIG. 7. Two-parameter bifurcation diagrams of the peak of  $P$  as a function of feedback strength,  $F_X$  ( $X = 1, 2, 3, 4$ ). Oscillations occur within the color region. In the white region, no oscillations occur. The color bar indicates the peak values of the oscillations derived from the corresponding parameter combinations of mode F3412.

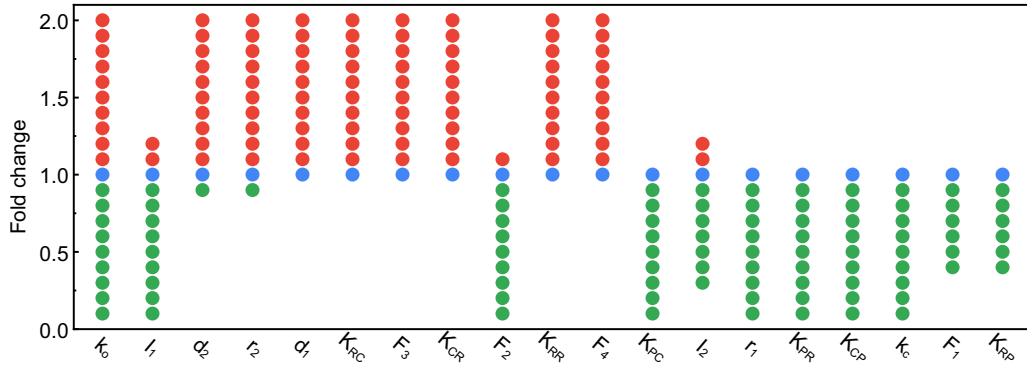


FIG. 8. Parameter sensitivity analysis. For each parameter, the circles depict the range of relative variation—expressed as a fold change of its standard value of mode F3412—in which oscillations are maintained.

increased to 0.6, corresponding to 0.1-fold to 1.2-fold of the standard value. From Fig. 8 we can see that for the majority of parameters, the oscillations only persist for a fold change either above or below 1. Two characteristics should be stressed here. First, the parameters corresponding to the numerator and denominator of a specific term in Eq. (1) have opposite trends. Second, except  $k_0$ , the parameters corresponding to the plus and minus term in each ODE of Eq. (1) have opposite trends. Overall, Fig. 8 indicates that the existence of oscillations is a rather robust property of the studied system and the parameter selection has a limited influence on it.

#### IV. DISCUSSION

The transient opening of PTP is responsible for many important physiological functions, while the persistent PTP opening is often associated with cell death. We thus hypothesize that, from a dynamical point of view, PTP opens in an oscillatory state under physiological conditions, whereas PTP opens in a high steady state under pathological conditions. It is well accepted that an increase in  $Ca^{2+}$  and ROS are triggers of PTP opening, and there are two positive feedback loops and two negative feedback loops in the  $Ca^{2+}$ -ROS-PTP system. It is not clear, however, how these feedback loops impact the dynamics of PTP opening. In view of the complexity brought about by the presence of the four feedback loops in this system, we construct a three-variable model to analyze the roles of each feedback loop in the oscillatory behavior of the PTP, and further to understand the interface between the physiological and pathological roles of the PTP.

In this study, we use two different approaches to address these questions. The first approach is to measure the robustness of the 12 theoretically possible oscillatory modes. The other approach is to apply bifurcation analysis to investigate the dynamics of mode F3412, which is possibly the most favorable circuit employed by biological systems due to its superb robustness in producing oscillations. The results obtained by the two approaches lead to four conclusions. First, the negative feedback loop, F3 or F4, is prerequisite for generating oscillations, while the positive feedback loop, F1 or F2, is necessary for maintaining robustness of the oscillations and elevating their peak values. Second, in terms of generating oscillations, F3 plays a more prominent role than F4, and F1 plays a more prominent role than F2. Third, F1 has a

dominant role in enhancing the robustness of the oscillations as well as in raising their peak values. Fourth, increasing the strength of negative feedbacks or decreasing that of positive feedbacks, not only promotes the occurrence of oscillations and thus protects the system against a high steady state, but also contributes to lowering the peak values of the oscillations.

On these bases, we propose a potential approach to the treatment of neurodegenerative diseases. The PTP dysregulation has been linked to the pathology of neurodegenerative diseases, where permanent PTP opening induces excessive cell death and brain tissue damage [6–9]. A proper decrease (or increase) in the strength of the two positive (or negative) feedback loops not only leads to a rightward shift of bifurcation point, broadening the oscillatory region (Fig. 5), but also makes the PTP in an oscillatory state, rather than in a high steady state (Fig. 6), which might improve cell survival and thus be beneficial in treating neurodegenerative diseases.

Although the transient opening of PTP is necessary for normal physiology, the persistent opening of PTP results in cell death. This makes us speculate that the transient opening with high activity may lead a cell to be on the verge of death. Thus, if a cell is to survive, it has to balance the trade-off between maintenance of oscillatory state of PTP opening and its oscillation peak, i.e., the oscillation peak values of PTP need to be tuned to an appropriate range. In this scenario, F1 and F3 constitute the core regulatory mechanism of oscillatory PTP opening. The existence of F3 is a prerequisite for PTP oscillations (Fig. 3), in accord with a long-standing view that PTP opening is a route for  $Ca^{2+}$  release from the mitochondria [51]. As for F1, on one hand, its existence is of critical importance in the maintenance of robustness of PTP oscillations (Fig. 3); on the other hand, F1 has a central role in raising the peak values of the oscillations [Figs. 3(c) and 7(a)]. A recent experiment demonstrated clearly that the ROS induced by  $Ca^{2+}$  signals exerts a positive feedback on  $Ca^{2+}$  release from the endoplasmic reticulum to mitochondria [28]. Taken together, the best strategy of an alive cell is to keep the activity of F1 and F3 and meanwhile to limit the activity of F1. Hence, our study identifies the key constraint and trade-off that a cell must deal with PTP opening in the struggle for life.

The two core feedback loops, F1 and F3, are centered on  $Ca^{2+}$ , which accounts for the role of  $Ca^{2+}$  as the master regulator of PTP opening [14]. The other two feedback loops, F2 and F4, which are centered on ROS, also have a regulatory

role in PTP oscillations and in maintaining their robustness. Previous theoretical works have shed light on the oscillatory robustness of a motif with interlinked positive and negative feedback loops. Tsai *et al.* established that adding a positive feedback loop to a repressilator, which is a cyclic triple negative feedback loop, can make the oscillators tunable and robust [47]. Ananthasubramaniam and Herzl used the Goodwin model to show that the benefits of two positive feedback loops are additive in a majority of the cases [52]. Nguyen extended the Goodwin model to reveal that dual negative feedback loops may provide robust tuning of the oscillation dynamics [53]. In the  $\text{Ca}^{2+}$ -ROS-PTP system, composed of a coherent feedforward loop and coupled feedback loops, the presence of F2 and F4 not only promotes the robustness of oscillations, but also increases the range of their amplitudes (Fig. 3), which is in agreement with the above views. In the light of evolutionary mechanisms we conjecture that the existence of F2 and F4 may act as a compensatory mechanism to regulate PTP opening when some mutations affect the feedback strength of F1 and/or F3. Thus, our study provides a rationale for the existence of the four feedback loops in the  $\text{Ca}^{2+}$ -ROS-PTP system.

Aside from  $\text{Ca}^{2+}$  and ROS, there are other modulators to regulate PTP opening, such as mitochondrial matrix pH, membrane potential, ADP/ATP balance, and Cyclophilin D, etc. [14]. Some previously published models have contributed to understanding the molecular mechanisms underlying PTP opening. Selivanov *et al.* developed one of the earlier models that described mitochondrial  $\text{Ca}^{2+}$ -induced  $\text{Ca}^{2+}$  release resulting from transient PTP opening, which is regulated by pH [54]. Bazil *et al.* constructed a bioenergetic model of the mitochondrial population undergoing persistent PTP opening, which mainly depends on  $\text{Ca}^{2+}$  and membrane potential [55]. Makarov *et al.* described the mitochondrial swelling dynamics [56] based on the modeling approach proposed earlier [54]. In the above three works, PTP opening dynamics is controlled by a threshold mechanism and acts as a module of the whole model. Quite recently, a modeling work focused on PTP opening dynamics by Wacquier *et al.* showed that the existence of a double-negative feedback loop between PTP opening and membrane potential leads the PTP to be a bistable switch: a small fraction of open PTP corresponds to the transient and low conductance mode, while a high value of this variable can be associated to the permanent and high conductance mode [57]. This is seemingly different from our results that an oscillatory state has relevance to the transient low-conductance opening mode, whereas a high steady state corresponds to the persistent high-conductance opening mode. Previous theoretical work has proved that a system with coupled positive and negative feedback loops can be tunable from monostability to bistability by increasing the strength of positive feedback, and can also undergo a transition from bistability to oscillation by increasing the strength of negative feedback [43]. Indeed, when changing the parameter values of the Wacquier model, the system can exhibit oscillatory behavior [57]. Taken together, the explicit mechanisms beneath PTP opening dynamics need to be explored in the future.

The experimental works demonstrating transient PTP opening raise a question on whether its opening period is fixed or varied, which may correspond to two distinct but interre-

lated mechanisms, i.e., deterministic or stochastic mechanism. It is noteworthy that, in a living cell, internal noise is ubiquitous and such noise makes all opening events appear to fluctuate randomly, even though the true underlying mechanism is deterministic. In this study we propose that the transient PTP opening caused by  $\text{Ca}^{2+}$  and ROS is inherently deterministic, but the stochastic mechanism may be also involved in this process. Mitochondrial superoxide flashes may reflect the stochastic nature of the transient PTP opening [58]. Song *et al.* recently developed a spatiotemporal model in which the PTP opening is assumed to be stochastic, which showed that the PTP opens briefly and keeps closed for most of the time [59]. Although this dynamic behavior can be produced by adjusting a parameter value for mode F3412 (Fig. S3), we only focus on the general dynamic properties of PTP oscillations, irrespective of their detailed dynamic behaviors. Moreover, although an alternative realization of the transient opening of PTP is the development of a stochastic version of a bistable model, as did in Ref. [57], the permanent opening of PTP can be hardly explained by this argumentation. Overall, the detailed dynamic behaviors of PTP opening need to be considered properly in future studies.

There are some modeling limitations that should be noted. First, the entry of  $\text{Ca}^{2+}$  into the mitochondria through MCU is actually in an oscillatory manner, but we treat it as a constant, representing the average influx rate during the opening of MCU. This is because we want to validate that PTP oscillations is an intrinsic property of the  $\text{Ca}^{2+}$ -ROS-PTP system, which is independent of the  $\text{Ca}^{2+}$  oscillations *per se*. Second, since the model is constructed at a coarse-grained level of description, it is described mainly by Hill functions. We acknowledge, however, that the robustness of oscillatory systems can be influenced by kinetic formulas. Third, in some situations, the PTP opening is involved in the ROS-induced ROS release. But we do not consider this in our model, because it may entangle the effects of F2 and F4.

Although we could not find detailed experimental data on the kinetics of  $\text{Ca}^{2+}$ , ROS, and PTP simultaneously to compare with our simulation results, such a simple model is sufficient to explore and understand the primary roles of the four feedback loops in PTP opening. The insights obtained from the simple model may be conserved in more complicated models, but are significantly harder to extract from these models. Based on these insights, future studies can focus on the detailed aspects to gain a better picture of the complex  $\text{Ca}^{2+}$ -ROS-PTP system. In addition, the present findings have at least two important implications. Our research will be informative in understanding and constructing the biochemical oscillatory circuits comprised of a coherent feedforward loop and coupled feedback loops. On the other hand, our study offers a therapeutic approach to the treatment of neurodegenerative diseases due to PTP dysregulation.

#### ACKNOWLEDGMENTS

This work was supported by National Natural Science Foundation of China (Grants No. 11504214, No. 11675134, No. 11874310, and No. 11871316), Scientific and Technological Innovation Programs of Higher Education Institutions in Shanxi (Grant No. 2019L0015), Shanxi Province Science Foundation for Youths (Grant No. 201901D211159).

- [1] M. Ott, V. Gogvadze, S. Orrenius, and B. Zhivotovsky, *Apoptosis* **12**, 913 (2007).
- [2] R. Rizzuto, D. De Stefani, A. Raffaello, and C. Mammucari, *Nat. Rev. Mol. Cell Biol.* **13**, 566 (2012).
- [3] L. Boyman, M. Karbowski, and W. J. Lederer, *Trends Mol. Med.* **26**, 21 (2020).
- [4] C. P. Baines *et al.* *Nature (London)* **434**, 658 (2005).
- [5] M. P. Murphy and R. C. Hartley, *Nat. Rev. Drug Discov.* **17**, 865 (2018).
- [6] H. Qi and J. Shuai, *Med. Hypotheses* **89**, 28 (2016).
- [7] M. H. Ludtmann *et al.* *Nat. Commun.* **9**, 2293 (2018).
- [8] C. Giorgi, S. Marchi, and P. Pinton, *Nat. Rev. Mol. Cell Biol.* **19**, 713 (2018).
- [9] P. Bernardi, A. Rasola, M. Forte, and G. Lippe, *Physiol. Rev.* **95**, 1111 (2015).
- [10] J. Q. Kwong and J. D. Molkentin, *Cell Metab.* **21**, 206 (2015).
- [11] L. K. Seidlmayer, V. V. Juettner, S. Kettlewell, E. V. Pavlov, L. A. Blatter, and E. N. Dedkova, *Cardiovasc. Res.* **106**, 237 (2015).
- [12] M. J. Pérez and R. A. Quintanilla, *Dev. Biol.* **426**, 1 (2017).
- [13] F. Ichas, L. S. Jouaville, and J.-P. Mazat, *Cell* **89**, 1145 (1997).
- [14] S. Hurst, J. Hoek, and S.-S. Sheu, *J. Bioenerg. Biomembr.* **49**, 27 (2017).
- [15] B. Wacquier, L. Combettes, and G. Dupont, *Cold Spring Harb. Perspect. Biol.* **11**, a035139 (2019).
- [16] T. M. Bauer and E. Murphy, *Circ. Res.* **126**, 280 (2020).
- [17] A. Rasola and P. Bernardi, *Cell Calcium* **50**, 222 (2011).
- [18] A. Agarwal, P.-H. Wu, E. G. Hughes, M. Fukaya, M. A. Tischfield, A. J. Langseth, D. Wirtz, and D. E. Bergles, *Neuron* **93**, 587 (2017).
- [19] L. Boyman, A. K. Coleman, G. Zhao, A. P. Wescott, H. C. Joca, B. M. Greiser, M. Karbowski, C. W. Ward, and W. J. Lederer, *Arch. Biochem. Biophys.* **666**, 31 (2019).
- [20] K. W. Kinnally, P. M. Peixoto, S.-Y. Ryu, and L. M. Dejean, *Biochim. Biophys. Acta* **1813**, 616 (2011).
- [21] S. Orrenius, V. Gogvadze, and B. Zhivotovsky, *Biochem. Biophys. Res. Commun.* **460**, 72 (2015).
- [22] E. Bertero and C. Maack, *Circ. Res.* **122**, 1460 (2018).
- [23] S. Kovac, A. Dinkova Kostova, A. Herrmann, N. Melzer, S. Meuth, and A. Gorji, *Int. J. Mol. Sci.* **18**, 1935 (2017).
- [24] O. Brandman and T. Meyer, *Science* **322**, 390 (2008).
- [25] R. S. Balaban, S. Nemoto, and T. Finkel, *Cell* **120**, 483 (2005).
- [26] G. S. Shadel and T. L. Horvath, *Cell* **163**, 560 (2015).
- [27] See Supplemental Material at <http://link.aps.org/supplemental/10.1103/PhysRevE.102.062422> for details on the biological background of the model, the robustness of the results, and the parameters of the model.
- [28] D. M. Booth, B. Enyedi, M. Geiszt, P. Várnai, and G. Hajnóczky, *Mol. Cell* **63**, 240 (2016).
- [29] N. Hempel and M. Trebak, *Cell Calcium* **63**, 70 (2017).
- [30] D. B. Zorov, M. Juhaszova, and S. J. Sollott, *Physiol. Rev.* **94**, 909 (2014).
- [31] L. Truong, Y.-M. Zheng, and Y.-X. Wang, *Arch. Biochem. Biophys.* **664**, 68 (2019).
- [32] N. Tajeddine, *Biochim. Biophys. Acta Gen Subj.* **1860**, 1079 (2016).
- [33] H. Rottenberg and J. B. Hoek, *Aging Cell* **16**, 943 (2017).
- [34] H. Qi, L. Li, and J. Shuai, *Sci. Rep.* **5**, 7984 (2015).
- [35] D. Chaudhuri, D. J. Artiga, S. A. Abiria, and D. E. Clapham, *Proc. Natl. Acad. Sci. USA* **113**, E1872 (2016).
- [36] Q. Zhang, S. Bhattacharya, and M. E. Andersen, *Open Biol.* **3**, 130031 (2013).
- [37] J. E. Ferrell Jr. and S. H. Ha, *Trends Biochem. Sci.* **39**, 612 (2014).
- [38] S. A. Frank, *Biol. Direct* **8**, 31 (2013).
- [39] K. M. Holmström and T. Finkel, *Nat. Rev. Mol. Cell Biol.* **15**, 411 (2014).
- [40] S. I. Dikalov, Y. F. Polienco, and I. Kirilyuk, *Antioxid. Redox Sign.* **28**, 1433 (2018).
- [41] B. Novák and J. J. Tyson, *Nat. Rev. Mol. Cell Biol.* **9**, 981 (2008).
- [42] J. E. Ferrell Jr., T. Y.-C. Tsai, and Q. Yang, *Cell* **144**, 874 (2011).
- [43] X.-J. Tian, X.-P. Zhang, F. Liu, and W. Wang, *Phys. Rev. E* **80**, 011926 (2009).
- [44] K. Maeda and H. Kurata, *J. Theor. Biol.* **440**, 21 (2018).
- [45] S. Busenberg and P. Vandendriessche, *J. Math. Anal. Appl.* **172**, 463 (1993).
- [46] W. Ma, L. Lai, Q. Ouyang, and C. Tang, *Mol. Syst. Biol.* **2**, 70 (2006).
- [47] T. Y.-C. Tsai, Y. S. Choi, W. Ma, J. R. Pomeroy, C. Tang, and J. E. Ferrell, *Science* **321**, 126 (2008).
- [48] H. Kitano, *Nat. Rev. Genet.* **5**, 826 (2004).
- [49] B. Hat, M. Kočańczyk, M. N. Bogdał, and T. Lipniacki, *PLoS Comput. Biol.* **12**, e1004787 (2016).
- [50] P. Pagliaro, F. Moro, F. Tullio, M.-G. Perrelli, and C. Penna, *Antioxid. Redox Sign.* **14**, 833 (2011).
- [51] P. Bernardi and S. von Stockum, *Cell Calcium* **52**, 22 (2012).
- [52] B. Ananthasubramaniam and H. Herzog, *PLoS ONE* **9**, e104761 (2014).
- [53] L. K. Nguyen, *J. R. Soc. Interface* **9**, 1998 (2012).
- [54] V. A. Selivanov, F. Ichas, E. L. Holmuhamedov, L. S. Jouaville, Y. V. Evtodienko, and J.-P. Mazat, *Biophys. Chem.* **72**, 111 (1998).
- [55] J. N. Bazil, G. T. Buzzard, and A. E. Rundell, *J. Theor. Biol.* **265**, 672 (2010).
- [56] V. Makarov, I. Khmelinskii, and S. Javadov, *Molecules* **23**, 783 (2018).
- [57] B. Wacquier, L. Combettes, and G. Dupont, *Sci. Rep.* **10**, 1 (2020).
- [58] T. Hou *et al.* *J. Biol. Chem.* **288**, 4602 (2013).
- [59] Z. Song, L.-H. Xie, J. N. Weiss, and Z. Qu, *Biophys. J.* **117**, 2349 (2019).